

P.306 TOWARDS INTEGRATED CLOUD MASK AND QUALITY CONTROL FOR ABI SST PRODUCT: PROTOTYPING WITH MSG/SEVIRI

N. Shabanov^{*1,2}, A. Ignatov¹, B. Petrenko^{1,2}, Y. Kihai³ and A. Heidinger^{1,4}

¹NOAA/NESDIS, Center for Satellite Applications and Research (STAR), Camp Springs, MD

²MSG Inc., Kensington, MD

³Perot Systems Government Services, Fairfax, VA

⁴University of Wisconsin, Madison, WI

1. INTRODUCTION

Geostationary Operational Environmental Satellite R-Series (GOES-R) will carry Advanced Baseline Imager (ABI) onboard. A suite of algorithms is currently being developed under the GOES-R Algorithm Working Group (AWG) for retrievals of environmental products including Sea Surface Temperature (SST) (Ignatov, 2009). The SST production system is based on the Advanced Clear-Sky Processor for Oceans (ACSP). It was initially developed for the Advanced Very High Resolution Radiometer (AVHRR) sensors flown onboard NOAA and MetOp polar-orbiting platforms (Liang et al., 2009, Petrenko et al., 2009) and subsequently adapted to process geostationary data from the Spinning Enhanced Visible and IR Imager (SEVIRI) onboard Meteosat Second Generation (MSG) platforms (Shabanov et al., 2009).

One key issue of the ABI SST product development is integration of the upstream ABI Cloud Mask (ABI CM) with SST-specific Quality Control (SST QC) to optimize the ABI SST product. In GOES-R, generic ABI CM will be evaluated for all imager pixels and made available for downstream products. Prior experience with AVHRR and MODIS suggests that a generic CM may not be optimal for all derived products, and product-specific QC may still be needed (Martins et al., 2002; Minnett and Evans, 2008; OS&I SAF SST, 2009). The approach adopted in the ABI CM is to provide a somewhat 'liberal' cloud screening, leaving product-specific QC up to retrieval algorithms (Heidinger, 2009).

This work reviews the structure of the ABI CM and SST QC, inter-compares their performance and seeks to identify areas for potential improvements of both. The ultimate objective is to optimally combine both ABI CM and SST QC for highly accurate and optimal SST product retrievals.

2. DATA

One day of Meteosat-9 (MSG-2) SEVIRI 15-minute Full Disk (FD) data for June 3, 2008 covering full diurnal cycle was analyzed in this study. The ABI CM and SST product (including SST QC) were generated and every other FD image was stored corresponding to 30-min

time intervals. FD image corresponds to a 3712x3712 pixel image, with 4.8 km resolution at nadir (Schmetz et al., 2002). The "SATELLITE" projection is used with the sensor positioned at (0.0;0.0) Lat/Lon position. SEVIRI FD primary input data include three Reflectance Channels (Ch1 centered @ 0.635 μm , Ch2 @ 0.810 μm , and Ch3 @ 1.640 μm) and three Thermal Channels (Ch4 @ 3.920 μm , Ch9 @ 10.80 μm , and Ch10 @ 12.00 μm), observation/illumination geometry and Land-Water mask.

Two major ancillary data sources include global weekly 1° fields of Reynolds SST (Reynolds et al., 2002) and the National Centers for Environmental Prediction Global Forecast System (NCEP/GFS) 1° 6-hour upper air data (Liang et al., 2009).

Currently, SST is retrieved using a regression split window NLSST algorithm (Walton et al., 1998). Other approaches based on using Community Radiative Transfer Model (CRTM) simulations in conjunction with first-guess SST and upper air fields are also being developed and tested.

3. ABI CLOUD MASK

Reliable clear-sky identification is critically important for accurate retrievals of clear-sky SST product. The ABI CM developed by the AWG Cloud Application Team at the University of Wisconsin builds upon heritage approaches employed for AVHRR, MODIS and SEVIRI (Heidinger, 2009). It includes up to 30 different tests, of which 10 are currently relevant to ocean applications (cf. Table 1). Thresholds in the individual ABI CM tests have been tuned against CALIPSO Lidar measurements. Online RTM (PFAAST) simulations are employed in several ABI CM tests (12, 13, 21, and 22, cf. Table 1). Target misclassification rate (False Clear + False Cloudy) is 13%. Latest tests over ocean demonstrated misclassification rate of 8.8% wrt CALIPSO data. The ABI CM output contains results of the individual cloud tests, which are further aggregated into overall ABI CM with four states: 'Confidently Clear', 'Probably Clear', 'Probably Cloudy', and 'Confidently Cloudy'. In order to facilitate comparison of ABI CM and SST QC in this study, the two 'Probably' categories were aggregated

and only three ABI CM categories were analyzed 'Clear', 'Probably' and 'Cloudy'.

4. SST QUALITY CONTROL

The objective of the SST QC is to assess the SST retrieval's accuracy, degraded by various environmental factors (possible contamination due to residual cloud, aerosols, sun glint, radiometric noise, extreme observation geometry, proximity to coast, etc). While ABI CM is relatively liberal to avoid misclassification of clear pixels as cloudy (false alarms), the QC is more conservative to avoid cloud leakage in the SST product. Thus, the implementation of the SST QC is different from ABI CM. It currently utilizes 5 tests (cf. Table 2). All tests (except 'Spatial Uniformity') rely on the CRTM simulations driven by *a priori* information (Reynolds SST and GFS upper atmosphere fields) (Liang et al., 2009). Significant reliance on *a priori* information is essential to meet high accuracy SST requirements, without significant reduction in the amount of clear-sky pixels. The SST QC output contains results of the individual QC tests, which are further aggregated into overall SST QC with three states: 'Best', 'Acceptable' and 'Poor'.

5. ANALYSES

The performance of the ABI CM and SST QC was intercompared and their impact on SST product assessed using: (1) side-by-side comparison of ABI CM and SST QC; (2) ABI CM vs. SST QC Confusion Matrix analysis; (3) Analysis of performance of individual ABI CM and SST QC tests.

5.1 SIDE-BY-SIDE COMPARISON OF ABI CM AND SST QC

Spatial distribution of ABI CM and SST QC is shown in Fig. 1 for one FD image at 12:00 UTC. As expected, QC is more conservative leaving fewer clear-sky pixels than the CM. Classes in the ABI CM are more clustered with clearly developed transitioning zones from 'Cloudy' through 'Probably' to 'Clear'. In contrast, the spatial pattern of the SST classes exhibits more random spikes, such that dominant class 'Poor' suppresses random contribution of minor classes when aggregating and displaying image.

Figure 2 shows time series of the components of ABI CM ('Clear', 'Probably' and 'Cloudy') and SST QC ('Best', 'Acceptable', and 'Poor'). Although the absolute values of clear-sky fraction identified by the ABI CM and SST QC are different, they both exhibit diurnal cycle with a minimum found at 03:00 UTC and maximum at 15:00 UTC (recall that the Meteosat is positioned at Greenwich meridian, so that the UTC time here is representative of the local observation time). Currently it still remains unclear if this observed diurnal cycle really reflects change in cloud cover during the course of the day, and what physical mechanism could be responsible for this change.

Overall, the fraction of 'Clear' CM pixels (17-21%) is larger than the fraction of 'Best' QC pixels (15-18%). Furthermore, the fraction of 'Probably' ABI CM pixels (~20%) is much larger than that of "Acceptable" SST QC pixels (~8%). Additional analysis (not shown) suggests that the pattern of ABI CM exhibits temporal discontinuities between day - night, and glint - no glint areas, while SST QC is more regular and continuous in time. In particular, the amount of "Cloudy" ABI CM pixels quickly builds up in the NW sector of the FD after 19:00 UTC. Another CM artifact is observed in the Saharan dust area, where highly reflective dust particles may be mistakenly classified as clouds during daytime (no misclassification takes place at night, when only thermal channels are used).

From Figs. 1-2 one concludes that the ABI CM is more 'liberal' than SST QC during whole diurnal cycle. This is acceptable for SST processing, as SST QC is envisioned to be applied on top of the ABI CM. However, temporal discontinuities and other miscellaneous artifacts (including buildup of cloudy pixels and Saharan dust misclassification) result in a loss of good SST pixels, which is unacceptable for SST users. The use of ABI aerosols mask should enhance capabilities of ABI CM data screening (Shoba, 2009)

Figures 3 and 4 quantify the impact of ABI CM and SST QC data screening on SST by showing SST deviations from the first-guess SST field, $\Delta T_s =$ retrieved Regression SST - reference Reynolds SST. Spatial patterns of ΔT_s in Fig. 3 are generally similar. In particular, both ABI CM and SST QC capture "hot spots" along the African coast and in the Mediterranean Sea, which are not captured by coarse resolution 1° Reynolds SST. However, residual cloud is more pronounced in the ABI CM (e.g., cold anomalies in the NW part of the Atlantic Ocean and in the Mediterranean Sea).

Results of statistical analysis of ΔT_s data screened with ABI CM and SST QC are shown in Fig. 4. In the case of ABI CM, cold tails of histograms are more pronounced. In the case of SST QC, the ΔT_s histogram is skewed on the right, suggesting a slight 'over-screening'. However, right shoulders of both histograms match very closely. Instantaneous values of mean and STD of ΔT_s statistics are indicated in the histograms and their diurnal cycle is shown separately. Mean ΔT_s is biased negative and shows more pronounced diurnal cycle compared to SST QC, suggesting more residual cloud contamination in ABI CM. This observation is further confirmed by the time series of standard deviations, which show that STDs for the ABI CM are a factor of ~3 larger than for SST QC. Figure 4 clearly indicates that the ABI CM alone is not sufficient to provide high accuracy SST retrievals, and additional SST QC is required.

5.2. CONFUSION MATRIX ANALYSIS

Confusion matrix analysis complements the side-by-side comparison of ABI CM and SST QC. Example of

confusion matrices are given in Table 3 for mid-day 12:00 UTC and near midnight 23:30 UTC. As a matter of convention, we consider SST QC as “Reference”. The rationale is that SST QC was specifically optimized for high-accuracy SST applications, and its superior performance for SST is independently confirmed in Fig. 5. In the confusion matrix we trace the following key components:

Both Clear = [QC=Best] \cap [CM=Clear],

False Cloudy = [QC=Best] \cap [CM=Probably || Cloudy],

False Clear = [QC=Acceptable || Poor] \cap [CM=Clear].

Consider the time series of the three components of the confusion matrix in Fig. 5. The majority of ABI CM “Clear” and SST QC “Best” pixels are consistent. As a result, the ‘Both Clear’ component comprises 9-16% of all ocean pixels. The ‘False Clear’ component is comparable to the ‘Both Clear’ sample and comprises 5-9% of all ocean pixels, indicating again that the ABI CM is liberal. This is acceptable for the SST applications, as SST QC will be applied on the top of the ABI CM and it will catch the residual cloud missed by the ABI CM. However, the ‘False Cloudy’ component comprises 3-4% of all ocean pixels, which is equivalent to ~18-25%, when compared to SST QC “Best” component. One approach to reduce ‘False Cloudy’ rate is to merge ‘Probably’ into ‘Clear’ category. In this case ‘False Cloudy’ rate will drop under 1%, but in expense of increasing factor of 2 of ‘False Clear’ component to 20%. Also note, discontinuities around 18:00 UTC in all three components are likely caused by residual glint effect.

Example spatial distribution of ΔT_s in the ‘False Clear’ and “False Cloudy” domains and the diurnal cycle of the corresponding ΔT_s statistics are shown in Fig. 7. Note that the statistics of the ‘Both Clear’ and ‘False Cloudy’ categories are close, indicating that these two categories are indistinguishable. On the other hand, the ‘False Clear’ ABI CM pixels form a distinct cluster with negative ΔT_s and large STD.

5.3. PERFORMANCE OF ABI CM AND SST QC INDIVIDUAL TESTS

Analyses of individual ABI CM and SST QC tests were performed to help identify those tests, whose adjustment is more likely to improve the SST product. Time series of data screening rate by individual ABI CM and SST QC tests are shown in Figs. 8 and 9, respectively. Unique feature of the SST QC tests is that their respective triggering rates are clustered together around 60-75%, suggesting that all QC tests are consistently tuned and work for SST screening. However, some tests may be performing redundant job. Measuring and reducing this redundancy is one of the future objectives towards refining the SST QC. In contrast, ABI CM individual tests have wide distribution of triggering rates. Triggering rates of thermal channels

based tests are flat through diurnal cycle with rate changing from 75% (“Thermal Uniformity”) to below 1% (“Uniform Low Stratus”). Reflectance based tests (“Reflectance Uniformity”, “Reflectance Gross Contrast”, “Relative Visible Contrast”, “4-micron emissivity”, and “Uniform Low Stratus”) have wide variation (0-60%) of triggering rates. Additionally, reflectance-based tests contribute to day-night and glint-no-glint discontinuities of the ABI CM.

As the minimization of “False Cloudy” category in ABI CM is the major task, consider Fig. 10 which shows contribution to the ‘False Cloudy’ rate to individual ABI CM tests, defined as follows,

Test Contribution = [Test= “ON”] \cap False Cloudy.

According to Fig. 10 “Thermal Uniformity” and “Reflectance Uniformity” tests are two major contributors to the ‘False Cloudy’ category. The relative contributions of the two tests exhibit a somewhat reciprocal character, i.e. the reflectance-based tests dominate during the daytime, whereas at night only thermal data are available.

Performance of individual tests with respect to reference SST is further shown in Figs. 11-12. An individual test separates all ocean pixels into two categories: definitely contaminated, and potentially clear (a mixture of clear and contaminated pixels). The analyses that follow were restricted to the first category. The following two metrics of ΔT_s over contaminated pixels (test was triggered ON) were considered: (a) spatial distribution; (b) histograms. We focus our analyses on most critical transitioning region of ΔT_s (-4,+4) [K] where contamination typically occurs.

First, consider results for the SST QC individual tests (Fig. 11). In the FD maps (top panels), performance of the individual tests is similar over thick cold clouds, which are well detected by most tests. The difference is mainly in how individual tests treat the ambient cloud and aerosol contamination. For instance, Saharan dust is detected by the ‘Radiance’, ‘Adaptive SST’, and ‘Static SST’ tests but not by the ‘Optical Depth’ and ‘SST Uniformity’ tests. The mask of the ‘SST Uniformity’ test is more fragmented compared to the others. ‘Adaptive SST’, ‘Optical depth’ and ‘SST Uniformity’ capture more ambient clouds than others as clearly seen by large proportion of pixels occupying the (-4,+4) [K] region on the FD images. Corresponding histograms of ΔT_s are shown in the bottom panels. Those plots show in the background distribution of ΔT_s over clear pixels (as identified by the total SST QC). In the foreground is shown the distribution of SST anomalies for the contaminated pixels. Ideal test should screen out cold tails and have minimal overlapping with the uncontaminated pixel distribution.. Note, ideal test initiates screening starting not from $\Delta T_s=0$ but from ΔT_s corresponding maximum of the ΔT_s histogram over clear pixels. The ‘Static SST’ test provides an example of such expected pattern. However in presence of

ambient cloud, aerosol contamination, glint effects, etc., the domains overlap (i.e., “Uniformity” and “Optical Depth” test). In general, substantial weight of the SST anomaly distribution at positive values may potentially suggest that the test needs fine-tuning (required, but not sufficient condition). Overall, according to the two metrics developed, all SST tests perform reasonably, but may require fine-tuning and minimizing redundancy.

Similar analyses have been also performed for the ABI CM individual tests (Fig. 12). Reflectance-based tests (“Reflectance Uniformity”, “Reflectance Gross Contrast”, and “Relative Visible Contrast”) introduce day-night discontinuity in the ABI CM. The two uniformity tests (“Reflectance Uniformity” and “Thermal Uniformity”) exhibit largest ΔT_s domain overlapping with the domain of uncontaminated pixels (similar results as for “Median Uniformity” SST QC test). Out of all thermal tests largest domain overlapping except of the mentioned above, exhibit ‘Emissivity of Tropopause’ and ‘Positive 4-5’ tests. The ‘Uniformity Low Stratus’ test has very low contribution rate and may be excluded in the future. Finally note that, none of the ABI CM tests screens out domain of the Sahara’s dust, which is well captured by several SST QC tests. This performance of the ABI CM is expected, as its focus is on the cloud detection, rather on many different types of data contamination/noise. Overall, in order to suite SST applications, ABI CM tests based only on thermal channels avoid day-night discontinuity, and they should be fine tuned.

5. CONCLUSIONS

1. The ABI CM performance evaluated wrt SST QC reference, meets the Cloud Mask ATBD specs (Heidinger, 2009). Total misclassification error wrt SST QC (False Cloudy + False Clear) is ~12% of all ocean pixels.
2. The rate of ‘False Clear’ is ~8-10% of all ocean pixels. The fact that CM is “liberal” is OK if ABI CM and SST QC are applied sequentially ABI CM over all pixels → SST QC over clear sky only). Pixels mistakenly identified as ‘Clear’ will be screened further by SST QC.

REFERENCES

- De Paepe B. et al., 2008: Aerosol retrieval over Ocean from SEVIRI for the use in GERB Earth’s radiation budget analysis, *RSE*, **112**, 2455-2468.
- Heidinger A., 2009: ABI Cloud Mask Algorithm Theoretical Basis.
- Ignatov A., 2009: ABI SST Algorithm Theoretical Basis Document.
- Le Borgne P. et al., 2006: Operational SST retrieval from MSG/SEVIRI data, EUMETSAT Meteorological Satellite Conference, 12-16 June 2006, Helsinki, Finland.
- Liang X. et al., 2009: Implementation of CRTM in ACSPO and validation against nighttime

3. The rate of ‘False Cloudy’ pixels is 3-4% of all ocean pixels. This constitutes 18-25% of the QC ‘Best’ domain. Further, major contributors to ‘False Cloudy’ are the uniformity tests, which work at the difficult mixed transition zones. This fact is the major restriction to implement sequential processing strategy.
4. Overall, the ABI CM has potentials for preliminary cloud screening upstream the ABI SST algorithm. However, further optimization of the ABI CM for SST requires adjustments or using different subsets of ABI CM tests.

6. FUTURE WORK

1. Repeat analysis over extended time series of data and sample all seasons to verify sustainability of performance and major conclusions.
2. Research on physical mechanism underlying seasonality of the amount of clear sky pixels over the diurnal cycle.
3. Analyze unique contribution and minimize redundancy of SST QC individual tests (i.e., combine and optimize tests).
4. Implement Thermal tests only version (exclude Reflectance tests) of the ABI CM to achieve CM continuity through the diurnal cycle. Optimize thresholds of the tests with objective to minimize ‘False Cloudy’ rate.
5. Test the feasibility of sequential processing of ABI CM and SST QC.

7. ACKNOWLEDGEMENT

The work is conducted under the Algorithm Working Group funded by GOES-R Program Office. Thanks to John Sapper, XingMing Liang, Feng Xu, John Stroup and Denise Frey of NOAA/NESDIS for helpful discussions. The views, opinions, and findings contained in this report are those of the authors and should not be construed as an official NOAA or US Government position, policy, or decision.

- radiance, *JGR*, **114**, D067112, doi:10.1029/2008JD010960 .
- Martins J. et al., 2002: MODIS cloud screening for remote sensing of aerosols over oceans using spatial variability, *GRL*, **29**(12), 8009, doi:10.1029/2001GL013252.
- Minnett, P., and R. Evans, 2008: Personal Communication.
- Petrenko, B., et al, 2009: Cloud Mask and Quality Control for SST within the ACSPO, AMS conference, Jan 11-15, 2009, Phoenix, AZ (poster JP1.12).
- Petrenko, B. et al., 2010: Clear-sky mask for ACSPO, *JTech*, in review.
- OS&I SAF SST Product User Manual, v2.1, Nov 2009.
- Schmetz J. et al, 2002: An Introduction to Meteosat Second Generation, *BAMS*, **83**, 977-992.

Shabanov N. et al, 2009: Prototyping SST retrievals from GOES-R ABI with MSG SEVIRI data. AMS Conf, Jan 11-15, 2009, Phoenix, AZ (poster JP1.12).

Walton C. et al, 2009: The development and operational application of nonlinear algorithms for the measurement of SSTs with the NOAA polar-orbiting environmental satellites. *JGR*, **103**, 27999- 28012.

Shobha K., 2009: ABI Aerosol Algorithm Theoretical Basis Document.

Table 1: Brief description of ABI Cloud Mask tests.

Test ID	Test Name	Description
09	RUT- Reflectance Uniformity Test	STD of the observed 0.6 μm reflectance within a 3x3 box surrounding each pixel checked against a globally fixed threshold (Reflectance analog of TUT).
10	TUT- Thermal Uniformity Test	STD of the observed 11 μm BT within a 3x3 box surrounding each pixel checked against a globally fixed threshold (Thermal analog of RUT).
11	RTCT- Relative Thermal Contrast Test	BT difference @ the 11 μm (Pixel minus Nearest Warm Center in 5x5 box) checked against a globally fixed threshold.
12	ENTROP- Emissivity at Tropopause.	Effective emissivity of a pixel is compared against a fixed threshold. For cloud at the tropopause, emissivity is elevated, while for clear sky it approaches 0.
13	PFMFT- Positive 4-5 Test	Split window test for semi-transparent cloud $\Delta\text{BT}=\text{BT}(11 \mu\text{m})-\text{BT}(12 \mu\text{m})$ is checked against the should precalculated ΔBT as a function of $\text{BT}(11 \mu\text{m})$.
16	RFMFT - Relative 4-5 Test	Split-window test. Significant deviations of pixel's ΔBT in 5x5 box from that at the NWC (positive or negative)are indicative of cloud.
17	RGCT - Reflectance Gross Contrast Test	Clouds exhibit large values of the visible reflectance compared to clear sky.
18	RVCT - Relative VIS Contrast Test	Relative VIS Contrast Test - over small region (3x3 box, cloud edge), cloudy pixels have largest contrast in VIS reflectance. Unlike RGCT, the RVCT test dynamically calculates its thresholds.
21	EMS4 – 3.9 μm Emissivity Test	3.9 μm emissivity for clouds is augmented, and near zero for clear sky.
22	ULST - Uniform Low Stratus Test	Low uniform stratus clouds are more reflective (less emissive) than the surface in the 3.9 μm . Test compares pixel emissivity with clear sky prediction @ Night.

Table 2: Brief description of SST Quality Control tests.

Test ID	Test Name	Description
01	Radiance Test	Checks for consistency between the observed BT @ 11 μm and 12 μm BT and those generated by CRTM for clear sky conditions.
03	Static SST Test	Detects unrealistically cold SST anomalies.
02	Adaptive SST Anomaly Test	Refines results of Static SST test, by analyzing statistics of clear/cloudy pixels within the neighborhood of the tested pixel.
05	Optical Depth Test	Checks optical depth generated by SST physical retrieval algorithm (high for clouds).
07	Spatial Uniformity Test	Detects fractional sub-pixel cloudiness by the presence of enhanced spatial variability in the retrieved SST.

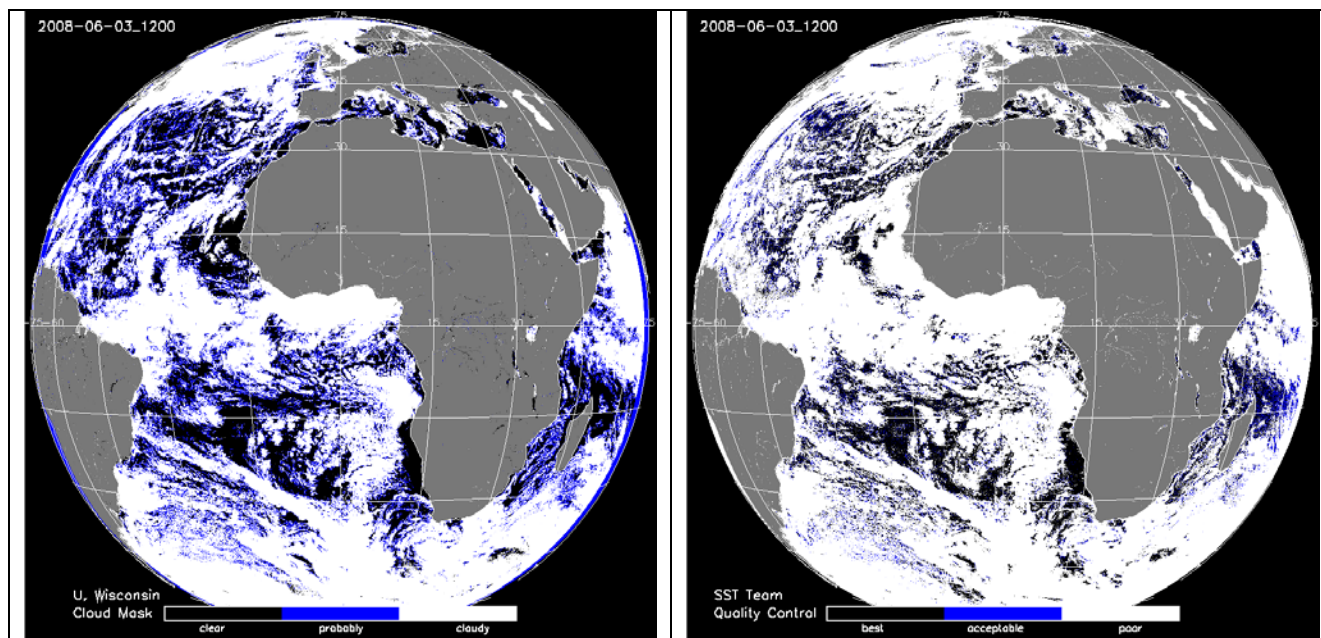


Fig. 1. Spatial distribution of ABI Cloud Mask (left) and SST Quality Control (right)- MSG-2 SEVIRI 15-min FD data at 12:00 UTC on June 03, 2008.

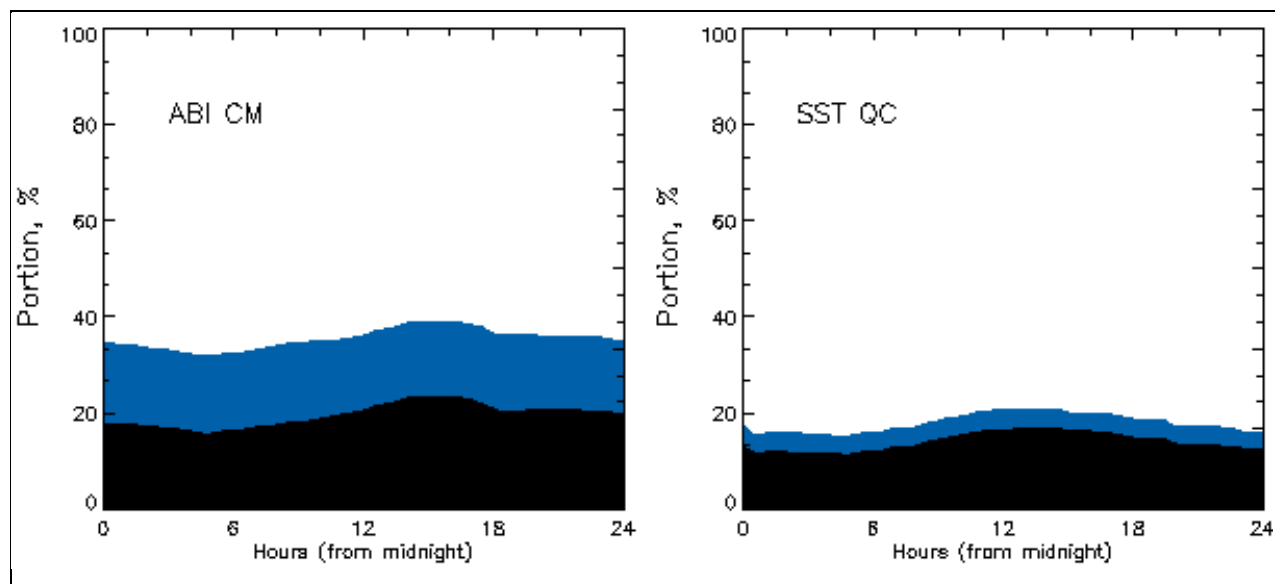


Fig. 2. Time series of the ABI CM (left) and SST QC (right) portion of retrieval states over whole diurnal cycle- MSG-2 SEVIRI 15-min FD data on June 03, 2008. Each portion is defined as the amount of pixels falling in the state normalized by total amount of ocean pixels.

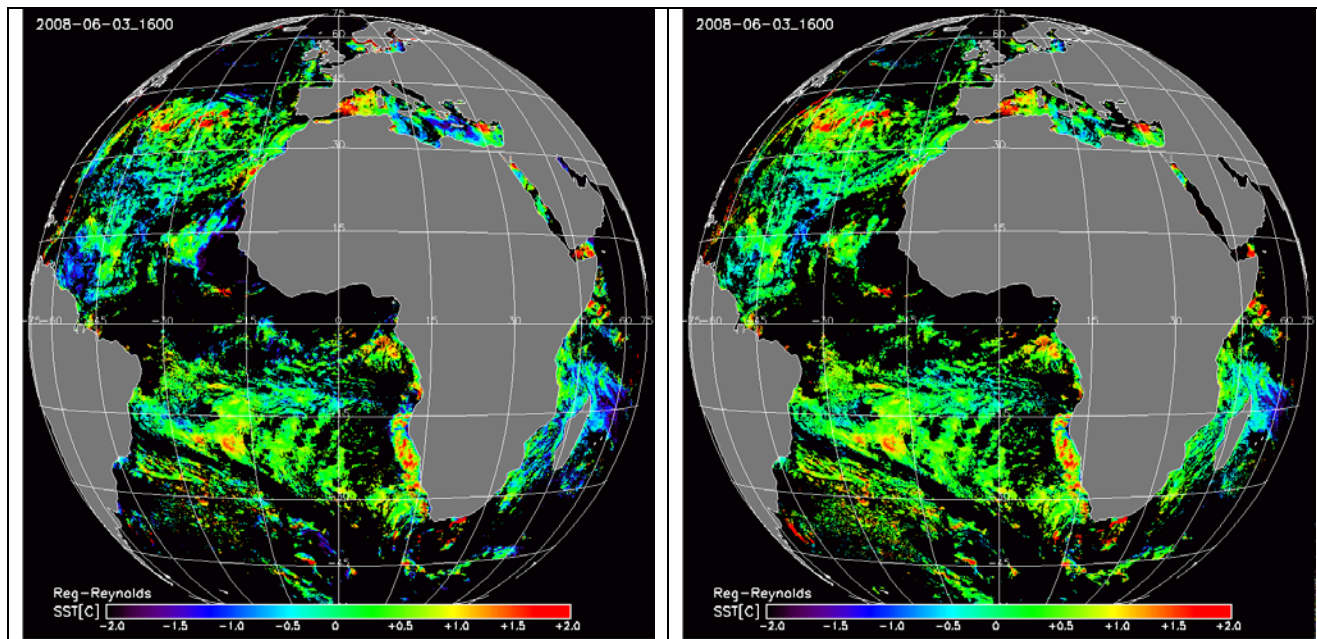


Fig. 3. Spatial distribution of ΔT_S (Regression SST – Reynolds SST) screened with ABI CM (left) and SST QC (right) masks- MSG-2 SEVIRI 15-min Full Disk (FD) data at 16:00 UTC on June 03, 2008.

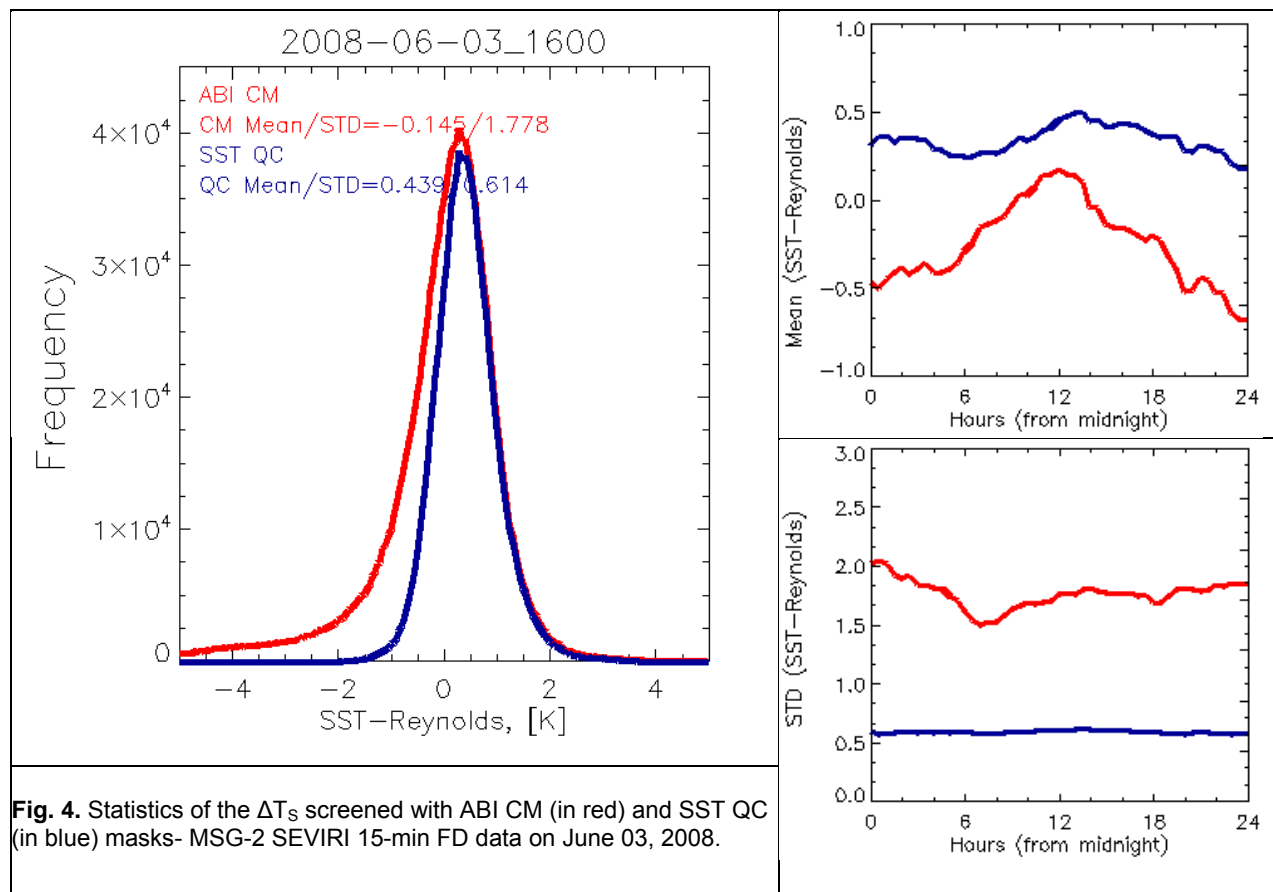


Fig. 4. Statistics of the ΔT_S screened with ABI CM (in red) and SST QC (in blue) masks- MSG-2 SEVIRI 15-min FD data on June 03, 2008.

Table 3: Confusion Matrix of ABI CM with respect to SST QC. Components of the matrix are given by the amount of pixels falling in each category normalized by the total amount ocean pixels. Color-coded are the following three components: 'False Clear' (red), 'False Cloudy' (blue), 'Both Clear' (red). Examples are for two FD images at 12:00 pm (a) and 0:30 (b) UTC on June 03, 2008.

	SST QC	Best	Accept	Poor
ABI CM	100%=	17.0% +	4.2% +	78.8% +
Clear	21.4% +	12.6%	1.8%	7.0%
Probably	15.6% +	3.7%	2.1%	9.9%
Cloudy	63.0% +	0.7%	0.4%	61.9%

a) 12:00 UTC

	SST QC	Best	Accept	Poor
ABI CM	100%=	12.7% +	3.7% +	83.6% +
Clear	20.1% +	9.9%	1.4%	8.8%
Probably	15.3% +	2.3%	1.9%	11.1%
Cloudy	64.5% +	0.5%	0.3%	63.8%

b) 0:30 UTC

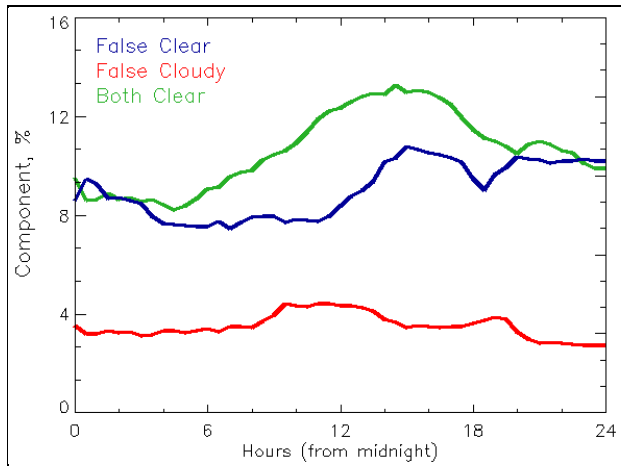


Fig. 5. Time series of the three components of the confusion matrix ('False Clear', 'False Cloudy', 'Both Clear') over diurnal cycle- MSG-2 SEVIRI 15-min FD data on June 03, 2008. Components are defined in Table 3.

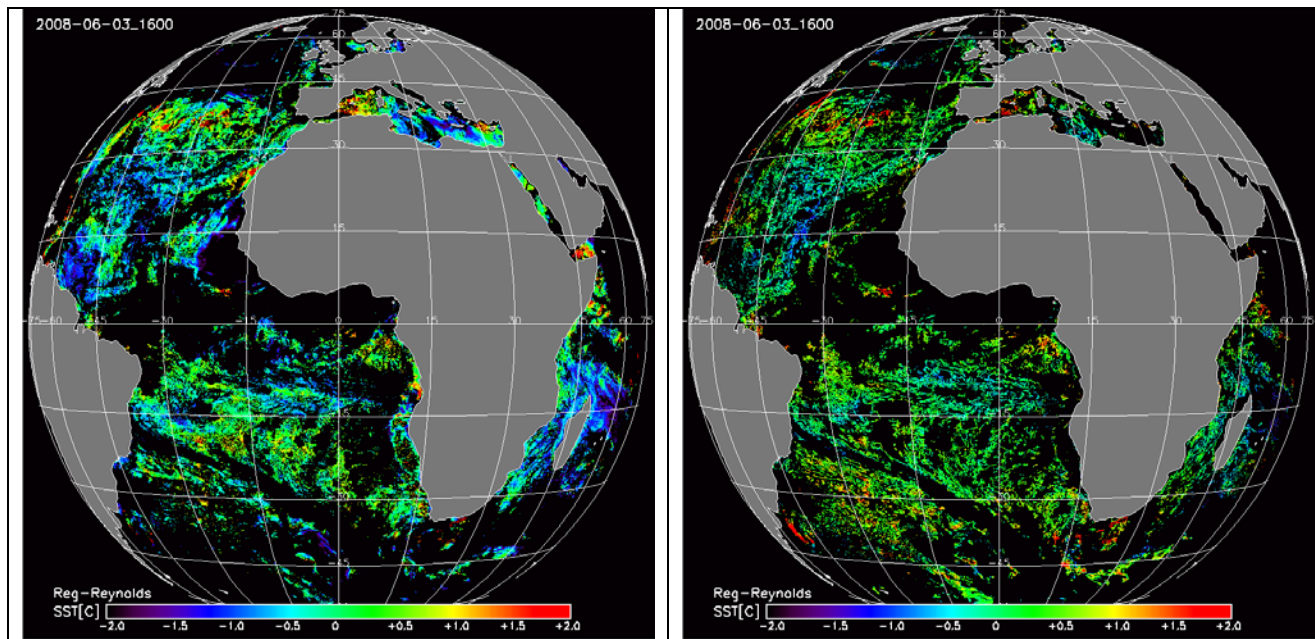


Fig. 6. Spatial distribution of ΔT_s (Regression SST – Reynolds SST) screened with ‘False Clear’ (left) and ‘False Cloudy’ (right) components of Confusion Matrix - MSG-2 SEVIRI 15-min Full Disk (FD) data at 16:00 UTC on June 03, 2008.

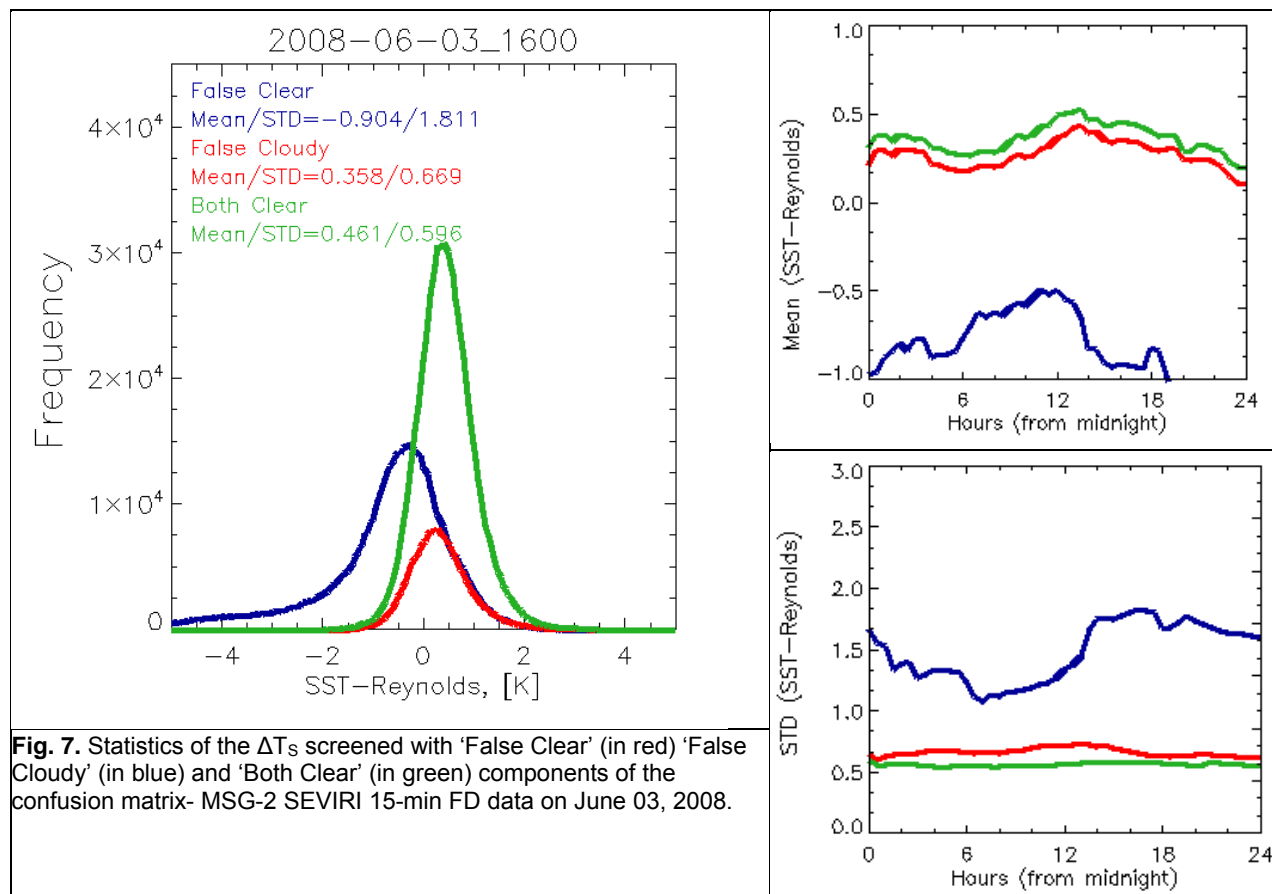


Fig. 7. Statistics of the ΔT_s screened with ‘False Clear’ (in red) ‘False Cloudy’ (in blue) and ‘Both Clear’ (in green) components of the confusion matrix- MSG-2 SEVIRI 15-min FD data on June 03, 2008.

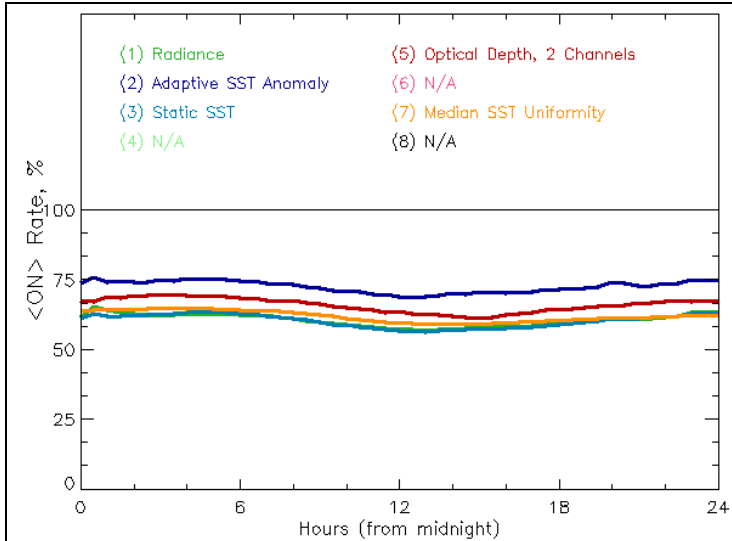


Fig. 8. Time series of data screening rate by individual SST QC tests over diurnal cycle- MSG-2 SEVIRI 15-min FD data on June 03, 2008.

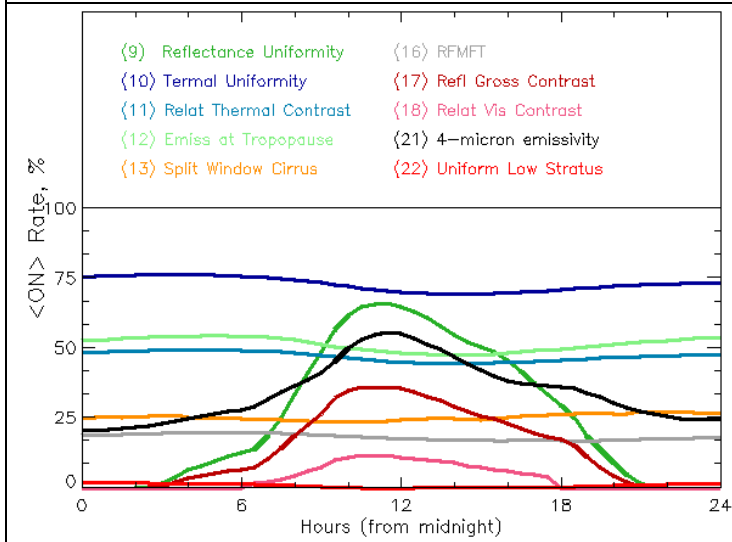


Fig. 9. Time series of data screening rate by individual ABI CM tests over diurnal cycle- the same data as in Fig. 8.

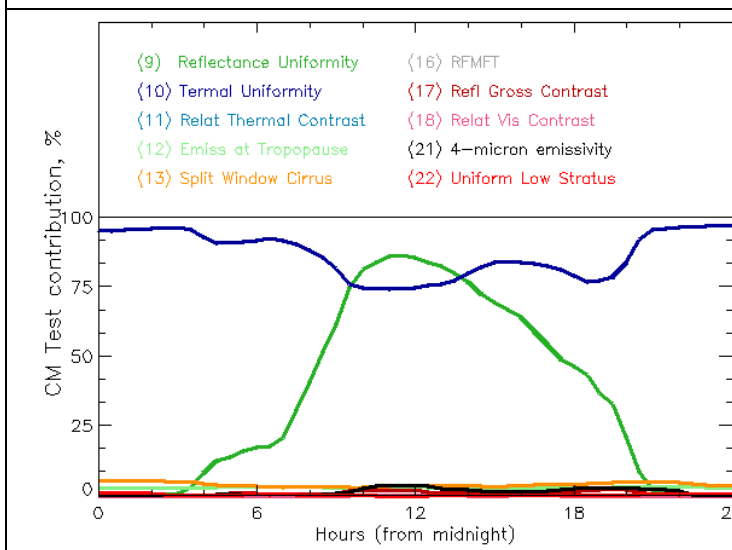


Fig. 10. Time series of contribution rate of individual ABI CM tests to False Cloudy component of Confusion Matrix over diurnal cycle- the same data as in Fig 8.

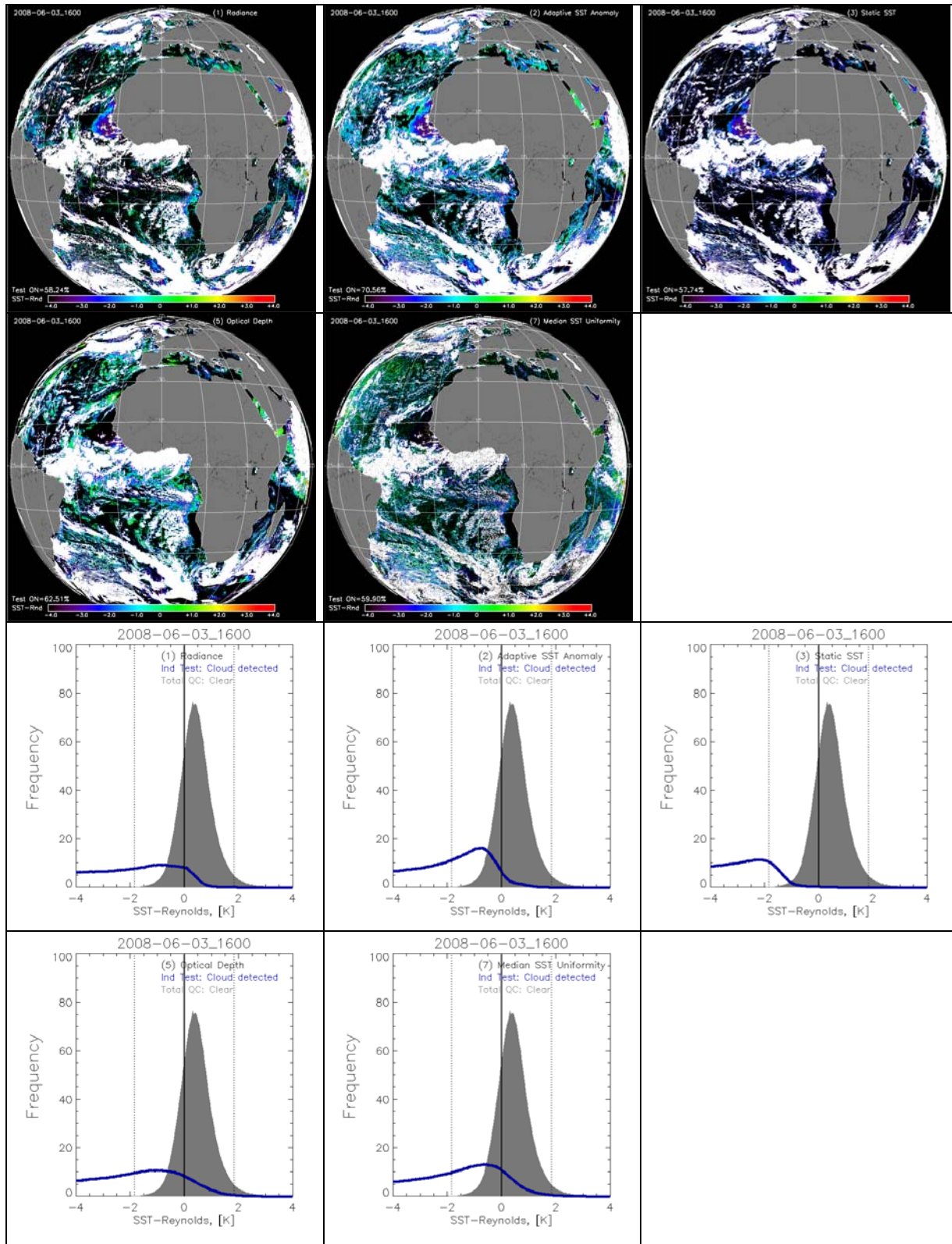


Fig. 11. Spatial distribution (top portion of the figure) and histograms (lower portion) of ΔT_S over contaminated pixels as detected by individual SST QC tests- MSG-2 SEVIRI 15-min FD data at 16:00 UTC on June 03, 2008.

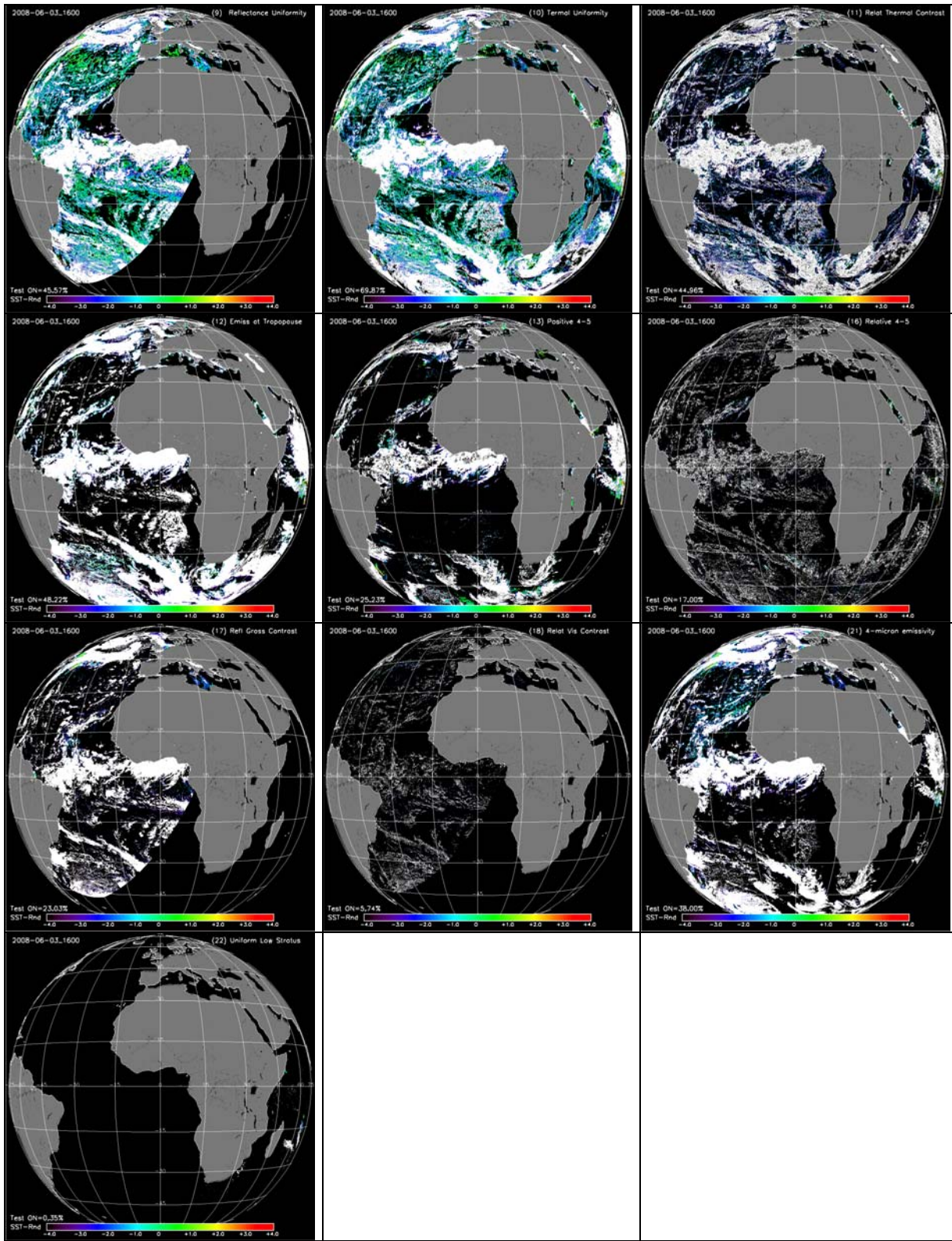


Fig. 12. To be continued.

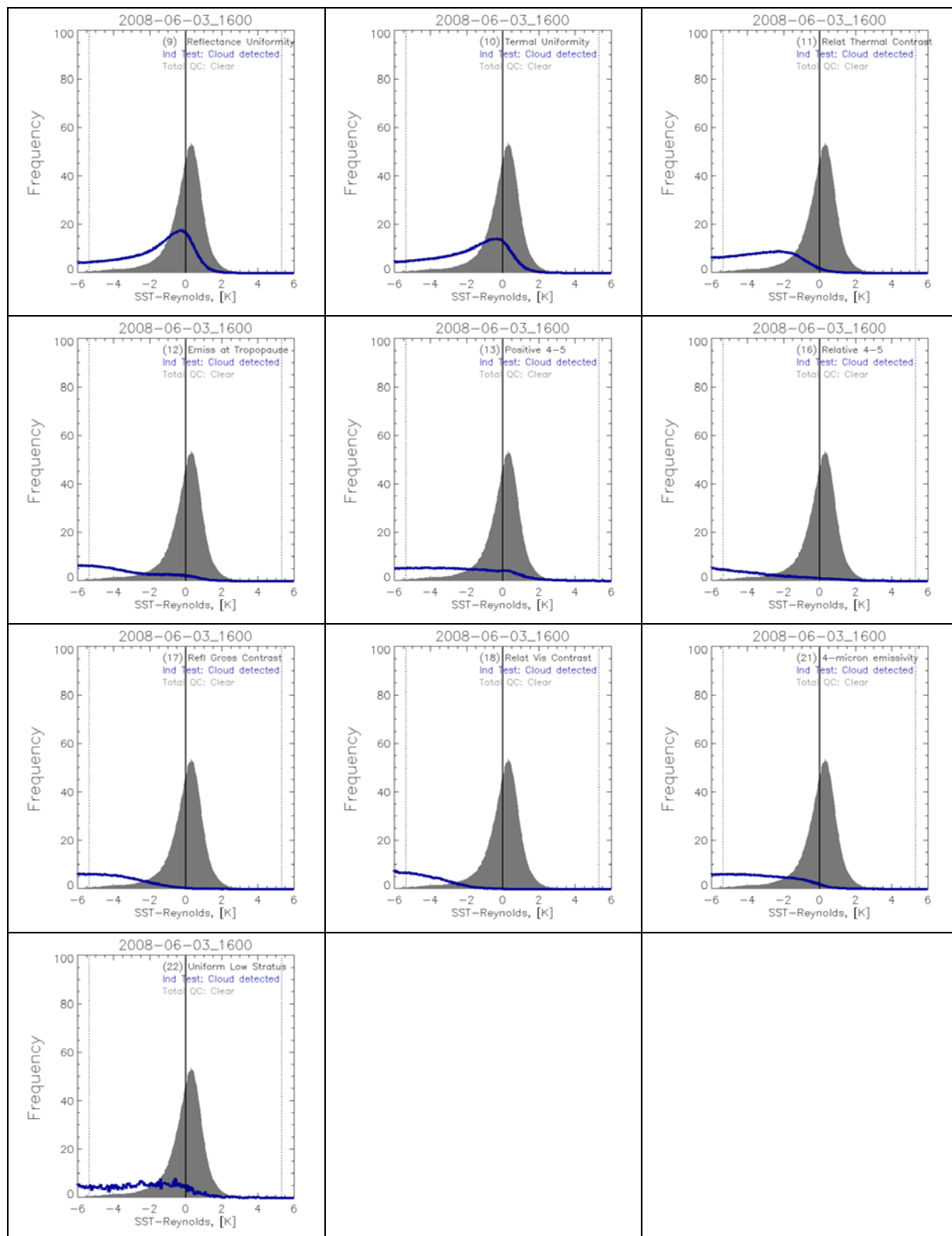


Fig. 12. (Continued). Spatial distribution (top portion of the figure) and histograms (lower portion) of ΔT_s over contaminated pixels as detected by individual ABI CM tests- MSG-2 SEVIRI 15-min FD data at 16:00 UTC on June 03, 2008.